7. Yang AS, Estécio MR, Doshi K et al (2004) A simple method for estimating global DNA methylation using bisulfite PCR of repetitive DNA elements. Nucleic Acids Res 32:e38
8. Ueda Y, Hiyama E, Kamimatsuse A et al (2011) Wnt signaling and telomerase activation of hepatoblastoma: correlation with chemosensitivity and surgical resectability. J Pediatr Surg 46:2221–2227
9. Yamada S, Ohira M, Horie H et al (2004) Expression profiling and differential screening between hepatoblastomas and the corresponding normal livers: identification of high expression of the PLK1 oncogene as a poor-prognostic indicator of hepatoblastomas. Oncogene 23:5901–5911
10. Agathanggelou A, Cooper WN, Latif F (2005) Role of the Ras-association domain family 1 tumor suppressor gene in human cancers. Cancer Res 65:3497–3508
11. Yang Q, Zage P, Kagan D et al (2004) Association of epigenetic inactivation of RASSF1A with poor outcome in human neuroblastoma. Clin Cancer Res 10:8493–8500
12. Ohshima J, Haruta M, Fujiwara Y et al (2012) Methylation of the RASSF1A promoter is predictive of poor outcome among patients with Wilms tumor. Pediatr Blood Cancer 59:499–505
13. Cairo S, Armengol C, De Reyniès A et al (2008) Hepatic stem-like phenotype and interplay of Wnt/beta-catenin and Myc signaling in aggressive childhood liver cancer. Cancer Cell 14:471–484

HEPATOLOGY
Official Journal of the American Association for the Study of Liver Diseases

Identification of Novel Serum Biomarkers of Hepatocellular Carcinoma Using Glycomic Analysis

Toshiya Kamiyama,[1] Hideki Yokoo,[1] Jun-Ichi Furukawa,[2] Masaki Kurogochi,[2] Tomoaki Togashi,[2] Nobuaki Miura,[2] Kazuaki Nakanishi,[1] Hirofumi Kamachi,[3] Tatsuhiko Kakisaka,[1] Yosuke Tsuruga,[1] Masato Fujiyoshi,[1] Akinobu Taketomi,[1] Shin-Ichiro Nishimura,[2] and Satoru Todo[3]

The altered *N*-glycosylation of glycoproteins has been suggested to play an important role in the behavior of malignant cells. Using glycomics technology, we attempted to determine the specific and detailed *N*-glycan profile for hepatocellular carcinoma (HCC) and investigate the prognostic capabilities. From 1999 to 2011, 369 patients underwent primary curative hepatectomy in our facility and were followed up for a median of 60.7 months. As normal controls, 26 living Japanese related liver transplantation donors were selected not infected by hepatitis B and C virus. Their mean age was 40.0 and 15 (57.7%) were male. We used a glycoblotting method to purify *N*-glycans from preoperative blood samples from this cohort (10 μL serum) which were then identified and quantified using mass spectrometry (MS). Correlations between the *N*-glycan levels and the clinicopathologic characteristics and outcomes for these patients were evaluated. Our analysis of the relative areas of all the sugar peaks identified by MS, totaling 67 *N*-glycans, revealed that a proportion had higher relative areas in the HCC cases compared with the normal controls. Fourteen of these molecules had an area under the curve of greater than 0.80. Analysis of the correlation between these 14 *N*-glycans and surgical outcomes by univariate and multivariate analysis identified G2890 (*m/z* value, 2890.052) as a significant recurrence factor and G3560 (*m/z* value, 3560.295) as a significant prognostic factor. G2890 and G3560 were found to be strongly correlated with tumor number, size, and vascular invasion. *Conclusion*: Quantitative glycoblotting based on whole serum *N*-glycan profiling is an effective approach to screening for new biomarkers. The G2890 and G3560 *N*-glycans determined by tumor glycomics appear to be promising biomarkers for malignant behavior in HCCs. (HEPATOLOGY 2013;57:2314-2325)

Hepatocellular carcinoma (HCC) is a common and fatal malignancy with a worldwide occurrence.[1] Liver resection has shown the highest level of control among the local treatments for HCC and is associated with a good survival rate.[2,3] However, the recurrence rates for HCC are still high even when a curative hepatectomy is performed.[4] Many factors associated with the prognosis and recurrence of HCC have now been reported. Vascular invasion of the portal vein and/or hepatic vein and tumor differentiation are important factors affecting survival and recurrence in HCC cases after a hepatectomy.[5,6] However, microvascular invasion and differentiation can only be detected by pathological examination just after a hepatectomy, and cannot be diagnosed preoperatively, and thus cannot be identified preoperatively either. Hence, the serum biomarkers alpha-fetoprotein (AFP) and protein induced by vitamin K absence-II (PIVKA-II) are used as prognostic markers[7,8] and also as surrogate markers for microvascular invasion and tumor differentiation.[9,10] AFP is associated with grade differentiation,[11] whereas PIVKA-II is related to vascular

Abbreviations: AFP, alpha-fetoprotein; AFP-L3, lens culinaris agglutinin-reactive fraction of alpha-fetoprotein; AUC, area under the curve; DFS, disease-free survival; HCC, hepatocellular carcinoma; ICGR15, indocyanin green retention rate at 15 minutes; PIVKA-II, protein induced by vitamin K absence or antagonism factor II; PS, patient survival; RF, risk factor; ROC, receiver operating characteristics.

From the [1]Department of Gastroenterological Surgery I, Hokkaido University Graduate School of Medicine, Hokkaido, Japan; [2]Graduate School of Life Science and Frontier Research Center for Post-Genome Science and Technology, Hokkaido University, Hokkaido, Japan; [3]Department of Transplantation Surgery, Hokkaido University Graduate School of Medicine, Hokkaido, Japan

Received May 8, 2012; accepted December 19, 2012.

Supported by grants for "Development of Systems and Technology for Advanced Measurement and Analysis (SENTAN)" from the Japan Science and Technology Agency (JST).

invasion.[12,13] However, these tumor markers have limited sensitivity and are less predictive than microvascular invasion,[14,15] which is the most potent determinant of recurrence and survival in HCC patients undergoing a hepatectomy.[5] Therefore, new biomarkers that are more strongly associated with prognosis and recurrence in HCC than AFP or PIVKA-II are highly desirable.

Glycosylation is one of the most common posttranslational protein modifications. Alterations in the *N*-glycosylation profiles of glycoproteins have been suggested to play important roles in the proliferation, differentiation, invasion, and metastasis of malignant cells. Glycan species can be analyzed and characterized using mass spectrometry (MS) and the profiling of these molecules when they are secreted or shed from cancer cells is also performed. Hence, some glycoproteins have been suggested as biomarkers of human carcinomas such as ovarian cancer, breast cancer, and HCC.[16-19] Of note, changes to the N-linked glycan modification of glycoproteins occur during the tumorigenesis and progression of HCC lesions. However, the correlation between the *N*-glycan profile and tumor-associated characteristics such as the degree of malignancy and prognosis has not been previously evaluated in HCC. Recently, we developed a novel glycomics method that facilitates high-throughput and large-scale glycome analysis using an automated glycan purification system, SweetBlot. This approach enables us to profile serum *N*-glycans quantitatively. Using this quantitative *N*-glycomics procedure by way of glycoblotting technology, which is both highly accurate and can be conducted on a large scale, we have previously evaluated the potential of using *N*-glycans as markers of the prognosis and recurrence of HCC.[20]

In our current study we evaluated preoperative blood samples from an HCC patient cohort from which we purified serum *N*-glycans using our glycoblotting method.[21,22] We performed *N*-glycan profiling using MS to search for factors related to prognosis and recurrence by analysis of patient outcomes in 369 consecutive HCC cases that had undergone a primary curative hepatectomy at our medical facility. Through this screen we sought to correlate *N*-glycan levels on glycoproteins with the clinicopathologic characteristics and the outcomes of HCC.

Patients and Methods

Patients. Between April 1999 and March 2011, 369 consecutive adult patients underwent a hepatectomy procedure for HCC at our center and this sample population was examined in the current study. Patients with extrahepatic metastases had been excluded from this cohort because the outcomes of a hepatectomy in these cases are typically very poor. The mean age of the patients in the final study group was 62.7 ± 10.6 years (range, 33-90), 301/369 (81.6%) cases were male, 176 (47.7%) were hepatitis B virus surface antigen-positive, 119 (32.2%) were hepatitis C virus antibody-positive, and 120 (32.5%) were designated as F4 based on the New Inuyama Classification system.[23] The preoperative serum AFP and PIVKA-II levels were simultaneously measured in the patients using standard methods at least 2 weeks before the hepatectomy at the time of the imaging studies. Among the 369 patients in the cohort, 358 (97.0%) were categorized as Child-Pugh class A. According to the TNM stage revised by the Liver Study Group of Japan in 2010,[24] 26 (7.0%) patients were in stage I, 172 (46.6%) in stage II, 111 (30.1%) in stage III, and 60 (16.3%) in stage IVA. The patients were followed up for a median of 60.7 months (range, 9.8-155.1). As a normal control group, 26 living related liver transplantation donors were selected. They were evaluated for eligibility as donors by liver function tests, measurements of the tumor markers AFP and PIVKA-II, and also by x-ray photographs of chest and abdomen and dynamic computed tomography (CT). Their mean age was 40.0 with a range of 20-48. Of 26 controls, 15 (57.7%) were male and 11 (42.3%) were female. All controls were Japanese and not infected by hepatitis B and C virus. This study was approved by the Institutional Review Board of the Hokkaido University, School of Advanced Medicine. Informed consent was obtained from each patient in accordance with the Ethics Committees Guidelines for our institution.

Experimental Procedures: Serum N-Glycomics by Way of Glycoblotting. *N*-glycans from serum samples were purified by glycoblotting using BlotGlycoH. These are commercially available synthetic polymer beads with high-density hydrazide groups (Sumitomo Bakelite,

Address reprint requests to: Toshiya Kamiyama, M.D., Department of Gastroenterological Surgery I, Hokkaido University Graduate School of Medicine, North 15, West 7, Kita-ku, Sapporo 060-8638 Japan. E-mail: t-kamiya@med.hokudai.ac.jp; fax: +81-11-717-7515.

View this article online at wileyonlinelibrary.com.
DOI 10.1002/hep.26262
Potential conflict of interest: Nothing to report.

Tokyo, Japan). All procedures used the SweetBlot automated glycan purification system containing a 96-well plate platform (System Instruments, Hachioji, Japan).

Enzymatic Degradation of Serum* N-*Glycans. Each 10-μL serum sample aliquot was dissolved in 50 μL of a 106-mM solution of ammonium bicarbonate containing 12 mM 1,4-dithiothreitol and 0.06% 1-propanesulfonic acid, 2-hydroxyl-3-myristamido (Wako Pure Chemical Industries, Osaka, Japan). After incubation at 60°C for 30 minutes, 123 mM iodoacetamide (10 μL) was added to the mixtures followed by incubation in the dark at room temperature to enable reductive alkylation. After 60 minutes, the mixture was treated with 200 U of trypsin (Sigma-Aldrich, St. Louis, MO) at 37°C for 2 hours, followed by heat-inactivation of the enzyme at 90°C for 10 minutes. After cooling to room temperature, the *N*-glycans were released from the tryptic glycopeptides by incubation with 325 U of PNGase F (New England BioLabs, Ipswich, MA) at 37°C for 6 hours.

N-*Glycan Purification and Modification by Glycoblotting.* Glycoblotting of sample mixtures containing whole serum *N*-glycans was performed in accordance with previously described procedures. Commercially available BlotGlyco H beads (500 μL) (10 mg/ml suspension; Sumitomo Bakelite) were aliquoted into the wells of a MultiScreen Solvinert hydrophilic PTFE (polytetrafluoroethlene) 96-well filter plate (EMD Millipore, Billerica, MA). After removal of the water using a vacuum pump, 20 μL of PNGase F-digested samples were applied to the wells, followed by the addition of 180 μL of 2% acetic acid in acetonitrile. The filter plate was then incubated at 80°C for 45 minutes to capture the *N*-glycans onto the beads by way of a chemically stable and reversible hydrazone bond. The beads were then washed using 200 μL of 2 M guanidine-HCl in 10 mM ammonium bicarbonate, followed by washing with the same volume of water and of 1% triethyl amine in methanol. Each washing step was performed twice. The *N*-glycan linked beads were next incubated with 10% acetic anhydride in 1% triethyl amine in methanol for 30 minutes at room temperature so that unreacted hydrazide groups would become capped by acetylation. After capping, the reaction solution was removed under a vacuum and the beads were serially washed with 2 × 200 μL of 10 mM HCl, 1% triethyl amine in methanol, and dioxane. This is a pretreatment for sialic acid modification. On-bead methyl esterification of carboxyl groups in the sialic acids was carried out with 100 μL of 100 mM 3-methyl-1-*P*-tolyltriazene (Tokyo Chemical Industry, Tokyo, Japan) in dioxane at 60°C for 90 minutes to dryness. After methyl esterification of the more stable glycans, the beads were serially washed in 200 μL of dioxane, water, 1% triethyl amine in methanol, and water. The captured glycans were then subjected to a *trans*-iminization reaction with BOA (O-benzylhydroxylamine) (Tokyo Chemical Industry) reagent for 45 minutes at 80°C. After this reaction, 150 μL of water was added to each well, followed by the recovery of derivatized glycans under a vacuum.

Matrix-Assisted Laser Desorption Ionization, Time-of-Flight (MALDI-TOF) and TOF/TOF Analysis. The *N*-glycans purified by glycoblotting were directly diluted with α-cyano-4-hydroxycinnamic acid diethylamine salt (Sigma-Aldrich) as ionic liquid matrices and spotted onto the MALDI target plate. The analytes were then subjected to MALDI-TOF MS analysis using an Ultraflex time-of-flight mass spectrometer III (Brucker Daltonics, Billerica, MA) in reflector, positive ion mode and typically summing 1,000 shots. The *N*-glycan peaks in the MALDI-TOF MS spectra were selected using FlexAnalysis v. 3 (Brucker Daltonics). The intensity of the isotopic peak of each glycan was normalized using 40 μM of internal standard (disialyloctasaccharide, Tokyo Chemical Industry) for each status, and its concentration was calculated from a calibration curve using human serum standards. The glycan structures were estimated using the GlycoMod Tool (http://br.expasy.org/tools/glycomod/), so that our system could quantitatively measure 67 *N*-glycans.

Hepatectomy. Anatomical resection is defined as a resection in which lesion(s) are completely removed on the basis of Couinaud's classification (segmentectomy, sectionectomy, and hemihepatectomy or more) in patients with a tolerable functional reserve. Nonanatomical partial, but complete resection was achieved in all of our cases. R0 resections were performed while the resection surface was found to be histologically free of HCC. The indocyanin green retention rate at 15 minutes was measured in each case to evaluate the liver function reserve, regardless of the presence or absence of cirrhosis.

HCC Recurrence. For the first 2 years after the hepatectomy procedure, the HCC patients in our cohort were monitored every 3 months using liver function tests, measurements of the tumor markers AFP and protein induced by PIVKA-II, and also by ultrasonography and dynamic CT. At 2 years postsurgery, routine CT was performed only once in 4 months. If recurrence was suspected, both CT and magnetic resonance imaging (MRI) were performed and, if necessary, CT during angiography and bone scintigraphy were undertaken.

Table 1. List of the 14 Serum N-Glycans That Were Evaluated to be Specific for Hepatocellular Carcinoma Compared with Normal Controls by Receiver Operating Characteristic (ROC) Analysis

N-glycans	m/z		Specificity (%)	Sensitivity (%)	Cutoff Value	AUC
G2032	2032.724	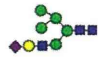	100	86.45	1.115	0.968
G2890	2890.052	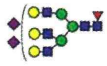	92.31	82.66	0.844	0.91
G1793	1793.672		92.31	75.61	1.963	0.9
G1708	1708.619		88.46	77.51	0.604	0.896
G1870	1870.672		88.46	75.88	2.886	0.873
G1955	1955.724		100	59.89	3.913	0.873
G3195	3195.163	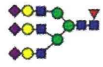	92.31	71.27	6.109	0.864
G3560	3560.295	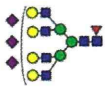	88.46	71.27	0.091	0.851
G2114	2114.778	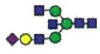	88.46	75.88	2.208	0.839
G1809	1809.666		84.62	72.9	0.679	0.838
G3341	3341.221	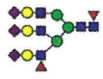	84.62	69.92	0.086	0.821
G1590	1590.592		80.77	69.92	10.696	0.817
G1362	1362.481		65.38	87.26	1.381	0.813
G3865	3865.407	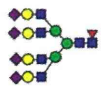	92.31	56.37	0.121	0.812

The area-under-the-curve (AUC) values of these 14 serum N-glycan were greater than 0.80. These glycan structures are represented with the symbol nomenclature explained in http://www.functionalglycomics.org/static/consortium/Nomenclature.shtml.

This enabled a precise diagnosis of the site, number, size, and invasiveness of any recurrent lesions.

Statistics. The specificity, the sensitivity, cutoff, and AUC (area under the curve) values of selected *N*-glycans are shown in Table 1. This ROC (receiver operating characteristics) analysis was carried out using R v. 2.12.1. The patient survival (PS) and disease-free survival rates (DFS) were determined using the Kaplan-Meier method and compared between groups by the log-rank test. Univariate analysis of variables was also performed, and selected variables using Akaike's Information Criterion (AIC)[25] were analyzed with the Cox proportional hazard model for multivariate analysis. Statistical analyses were performed using

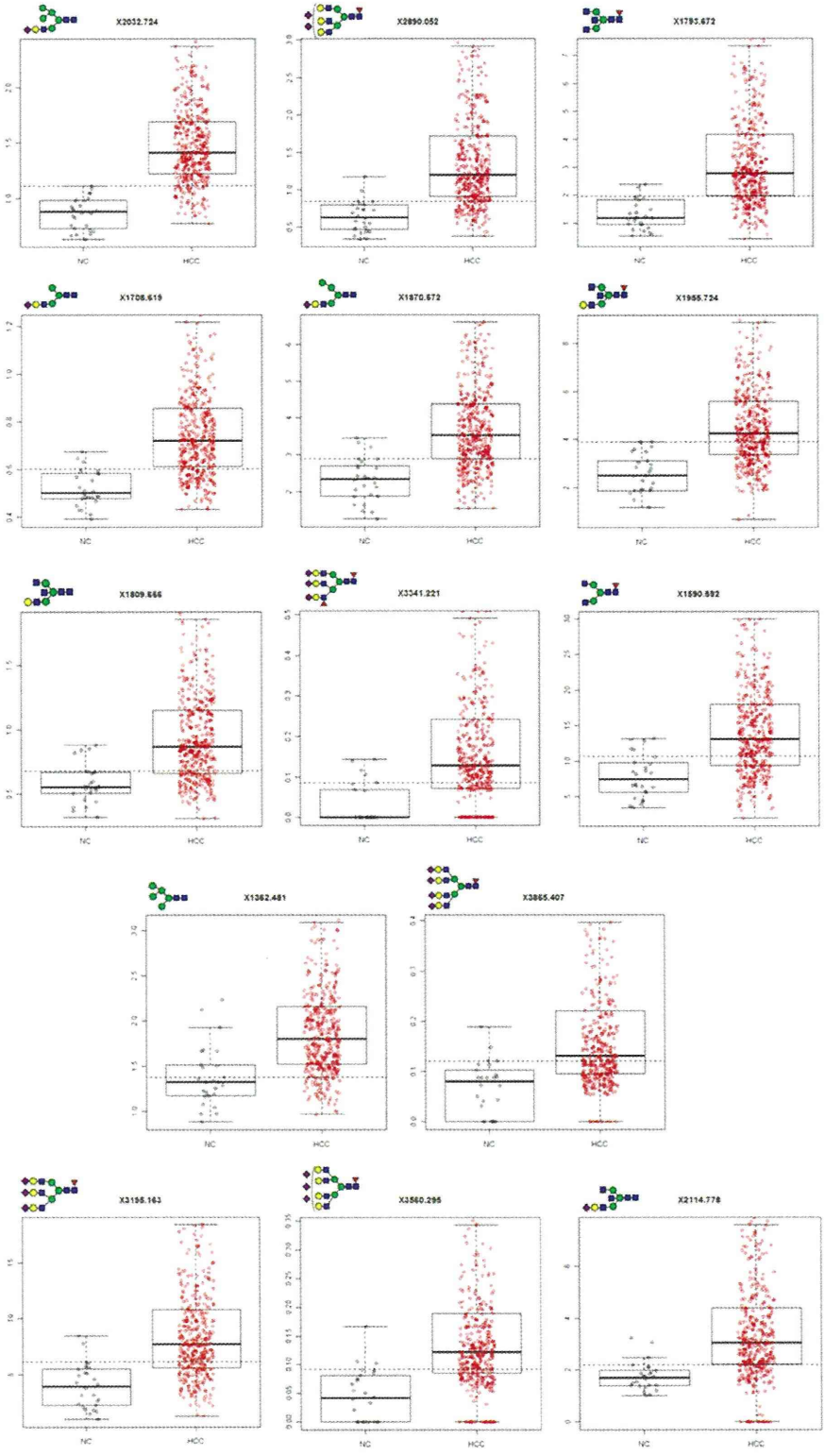

Fig. 1. Boxplots of the disease-free individuals (NC) and HCC patients for the selected 14 *N*-glycans. The dotted lines in the graphs represent the cutoff values determined in this analysis. These graphs were drawn using R v. 2.12.1.

Table 2. Univariate Analysis of Predictive Values (the Selected 14 *N*-Glycans) of Patient Survival (PS) and Disease-Free Survival (DFS)

		(n)	PS Hazard Ratio	PS *P*-value	DFS Hazard Ratio	DFS *P*-value
G2032	Low	206	1	0.9362	1	0.1054
	High	163	1.017		1.243	
G2890	Low	152	1	<0.0001	1	0.0001
	High	217	3.044		1.705	
G1793	Low	112	1	0.6829	1	0.2897
	High	257	1.095		1.168	
G1708	Low	145	1	0.0016	1	0.0043
	High	224	2.017		1.485	
G1870	Low	151	1	0.5552	1	0.4008
	High	218	1.132		1.122	
G1955	Low	113	1	0.4213	1	0.795
	High	256	1.2		1.038	
G3195	Low	206	1	<0.0001	1	0.0001
	High	163	3.238		1.662	
G3560	Low	246	1	<0.0001	1	<0.0001
	High	123	4.209		1.74	
G2114	Low	275	1	0.0056	1	0.1627
	High	94	1.776		1.232	
G1809	Low	238	1	0.0027	1	0.055
	High	131	1.824		1.306	
G3341	Low	188	1	<0.0001	1	0.0005
	High	181	3.185		1.592	
G1590	Low	167	1	0.0956	1	0.9102
	High	202	1.413		0.985	
G1362	Low	261	1	0.0399	1	0.0004
	High	108	1.526		1.634	
G3865	Low	192	1	<0.0001	1	0.0014
	High	177	3.145		1.532	

standard tests (χ^2, *t* test) where appropriate using StatView 5.0 for Windows (SAS Institute, Cary, NC). Significance was defined as $P < 0.05$.

Results

Profiling of Human Serum Glycoforms and ROC Analysis in HCC Patients and Normal Controls. *N*-glycan profiles of blood samples from our HCC cohort were obtained by MALDI-TOF MS analysis using the high-throughput features of the instrument. We thereby identified 67 *N*-glycans from which we selected molecules that showed statistical differences by ROC analysis between HCC and disease-free individuals (normal controls, NC) comprising living related liver transplantation donors. Glycans with an AUC value greater than 0.80 were selected for analysis (Table 1) and boxplots for these selected molecules (14 in total) are shown in Fig. 1. Clear differences in the distribution of these factors are evident between the NC and HCC patients. The cutoff values were determined using the maximum values for specificity plus sensitivity. G2890 was elevated more than a cutoff value in 305 (82.7%) of HCC patients and G3560 in 261 (70.7%).

Causes of Death. There were 115 deaths in total among our 369 HCC patient cohort (31.2%). The causes of death were as follows: HCC recurrence (n = 97; 84.3%), liver failure (n = 6; 5.2%), and other causes (n = 12; 10.4%).

Univariate Analysis and Multivariate Analysis of Overall Patient and Disease-Free Survival. The overall PS rates at 1, 3, and 5 years in our HCC cohort were 88.8%, 76.4%, and 67.6%, respectively. The DFS values for this groups at 1, 3, and 5 years were 64.0%, 35.5%, and 27.4%, respectively. The 14 serum N-glycans that were highly specific for HCC were evaluated for 3-year recurrence-free survival by ROC analysis to determine the cutoff values about these N-glycans. The patients were divided to two groups by these cutoff values. The PS and DFS measurements associated with the selected 14 selected *N*-glycans were evaluated by univariate analysis. The *P* values for the PS rates associated with G2890, G1708, G3195, G3560, G2114, G1809, G3341, G1362, and G3865 were all less than 0.05. The DFS *P* values for G2890, G1708, G3195, G3560, G3341, G1362, and G3865 were also less than 0.05 (Table 2). When clinical and tumor-associated factors were evaluated by univariate analysis, albumin, Child-Pugh classification,

Table 3. Univariate Analysis of Predictive Values (Clinical and Tumor Associated Factors) for Patient Survival (PS) and Disease-Free Survival (DFS)

		(n)	PS Hazard Ratio	PS *P*-value	DFS Hazard Ratio	DFS *P*-value
Sex	Male	301	1	0.7486	1	0.6535
	Female	68	0.913		0.943	
Age (years)	<=62	160	1	0.3272	1	0.6320
	62<	209	1.211		1.106	
HBV	Positive	176	1.259	0.1911	1.007	0.8093
	Negative	192	1		1	
HCV	Positive	119	1.291	0.2433	1.008	0.8183
	Negative	250	1		1	
Albumin (mg/dL)	<=4.05	147	2.128	<0.0001	1.626	0.0001
	4.05<	222	1		1	
Total bilirubin (mg/dL)	<=0.82	235	1	0.5831	1	0.5241
	0.82<	134	1.122		1.128	
ICGR15 (%)	<=16.7	223	1	0.1223	1	0.0106
	16.7<	146	1.349		1.375	
Child-Pugh	A	358	1	<0.0001	1	0.0374
	B	11	4.292		2.169	
Anatomical resection	Anatomical	282	1	0.8569	1	0.1435
	Nonanatomical	87	0.949		1.225	
AFP (ng/mL)	<=20	183	1	<0.0001	1	0.0008
	20<<=1000	115	2.395		1.449	
	1000<	71	4.433		1.870	
AFP-L3 (%)	<=15	255	1	<0.0001	1	0.0567
	15<	113	2.366		1.285	
PIVKA-II (mAU/mL)	<=40	109	1	<0.0001	1	0.0095
	40<<=1000	133	1.593		1.240	
	1000<	123	3.784		1.635	
Number	Single	235	1	<0.0001	1	<0.0001
	2,3	89	3.731		2.252	
	4<=	45	7.299		3.788	
Size (cm)	<=3	116	1	<0.0001	1	0.0086
	3<<=5	96	2.688		1.260	
	5<	157	4.049		1.570	
Differentiation	Well	17	1	0.0003	1	0.0002
	Moderately	190	2.568		2.990	
	Poorly	159	5.358		4.361	
Vp	Positive	94	4.630	<0.0001	2.156	<0.0001
	Negative	275	1		1	
Vv	Positive	35	5	<0.0001	1.969	0.0004
	Negative	334	1		1	
Macroscopic vascular invasion	Positive	48	6.135	<0.0001	1.961	<0.0001
	Negative	321	1		1	
Stage	1	26	1	<0.0001	1	<0.0001
	2	172	2.844		1.206	
	3	111	9.901		2.404	
	4A	60	15.625		3.106	
Noncancerous liver	Cirrhosis	120	1.199	0.3105	1.293	0.0398
	Noncirrhosis	249	1		1	

AFP, alpha-fetoprotein; PIVKA-II, protein induced by vitamin K absence or antagonism factor II; AFP-L3, lens culinaris agglutinin-reactive fraction of alpha-fetoprotein; vp, microscopic tumor thrombus in the portal vein; vv, microscopic tumor thrombus in the hepatic vein; HBV, hepatitis B virus s antigen; HCV, anti-hepatitis C virus antibody; ICGR15, indocyanin green retention rate at 15 minutes.

AFP, AFP-L3 (lens culinaris agglutinin-reactive fraction of alpha-fetoprotein), PIVKA-II, tumor number, tumor size, differentiation, microscopic portal vein invasion, microscopic hepatic vein invasion, macroscopic vascular invasion, and stage were found to be significantly associated with the PS rate. When the same analysis was undertaken for the DFS rate by univariate analysis, albumin, indocyanin green retention rate at 15 minutes, Child-Pugh classification, AFP, PIVKA-II, tumor number, tumor size, differentiation, microscopic portal vein invasion, microscopic hepatic vein invasion, macroscopic vascular invasion, stage, and noncancerous liver were found to be significantly associated with this measure (Table 3).

The variable selection from 19 clinical and tumor-associated factors in Table 3 and the 14 serum

Table 4. Multivariate Analysis of Values That Is Predictive for Overall HCC Patient Survival

		P	Hazard Ratio	95% Confidence Interval	
ICGR15 (%)	16.7<	0.000209	2.435	1.5213	3.898
Child-Pugh	B	0.011136	3.007	1.2852	7.037
AFP (ng/mL)	20<<=1000	0.0003	2.558	1.5372	4.256
	1000<	0.000217	2.782	1.6177	4.786
Tumor number	2,3	0.011844	1.937	1.1575	3.241
	4<=	<0.0001	2.989	1.7693	5.049
Size (cm)	3<<=5	0.278625	1.483	0.7269	3.026
	5<	0.016071	2.237	1.1613	4.307
Vp	Positive	<0.0001	2.982	1.8446	4.822
C3560	>0.158	<0.0001	2.52	1.6191	3.923

ICGR15, indocyanin green retention rate at 15 minutes, AFP, alpha-fetoprotein; vp, microscopic tumor thrombus in the portal vein.

Table 5. Multivariate Analysis of Values That Are Predictive of Disease-Free Survival in HCC Patients

		P	Hazard Ratio	95% Confidence Interval	
ICGR15 (%)	16.7<	0.00334	1.519	1.149	2.008
AFP (ng/mL)	20<<=1000	0.04904	1.366	1.001	1.864
	1000<	0.01851	1.591	1.081	2.342
Tumor number	2,3	0.0072	1.551	1.126	2.135
	4<=	<0.0001	2.649	1.704	4.118
Differentiation	Moderately	0.01495	2.838	1.225	6.577
	Poor	0.00501	3.398	1.446	7.984
vp	Positive	0.01023	1.544	1.108	2.152
C2890	>1.12	0.01125	1.443	1.087	1.915

ICGR15, indocyanin green retention rate at 15 minutes, AFP, alpha-fetoprotein; vp, microscopic tumor thrombus in the portal vein.

N-glycans using the AIC was performed and the selected valuables were analyzed with PS and DFS by multivariate analysis. G3560 were found to be independent risk factors for PS (Table 4) and G2890 for DFS (Table 5).

The PS rates of HCC cases with low serum G3560 levels at 5 years were 80.5% and of high serum G3560 at 5 years were 40.4%. The DFS outcomes associated with low and high serum G2890 levels at 5 years were 21.3% and 35.1%, respectively (Fig. 2).

Relationship Between Clinical and Tumor-Associated Factors in HCC and Specific Glycans. Among the low and high G2890 HCC groups, there were significant differences found in a number of clinical and tumor-associated factors including albumin, Child-Pugh classification, AFP, PIVKA-II, tumor number, tumor size, microscopic portal vein invasion, microscopic hepatic vein invasion, macroscopic vascular invasion, and stage (Table 6). In comparing the low and high G3560 HCC patients, significant differences were found in albumin, Child-Pugh Classification, operative procedures, AFP, AFP-L3, PIVKA-II, tumor number, tumor size, differentiation profiles, microscopic portal vein invasion, microscopic hepatic vein invasion, macroscopic vascular invasion, and stage (Table 6).

Discussion

The *N*-glycan profiles of a large cohort of HCC patients were obtained in our current study by MALDI-TOF MS analysis and 67 of these molecules were thereby quantified. Of this group of factors, 14 *N*-glycans showed higher relative peaks in the HCC patients compared with normal controls and were

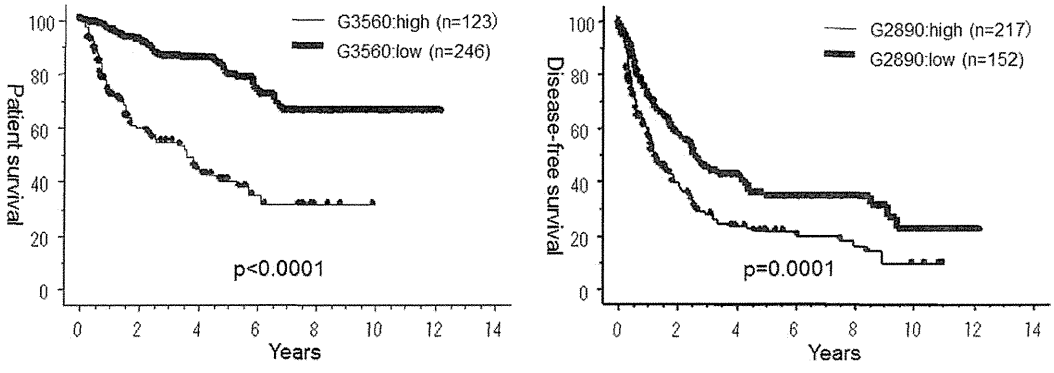

Fig. 2. The PS rates of HCC cases with low and high serum G3560 levels at 5 years were 80.5% and 40.4%, respectively. The DFS outcomes associated with low and high serum G2890 levels at 5 years were 21.3% and 35.1%, respectively.

Table 6. Correlation Between the G2890 and G3560 *N*-Glycans and Clinical and Tumor Associated Factors in HCC Cases

		G2890			G3560		
		High (n=217)	Low (n=152)	P	High (n=123)	Low (n=246)	P
Sex	Male	184	117	0.0767	105	196	0.2286
	Female	33	35		18	50	
Age	≦62	90	70	0.4433	49	111	0.393
	>62	127	82		74	135	
HBV	Positive	107	69	0.5254	59	117	0.9706
	Negative	110	83		64	129	
HCV	Positive	63	56	0.1425	32	87	0.0904
	Negative	154	96		91	159	
Albumin (mg/dL)	≦4.05	109	38	<0.0001	73	74	<0.0001
	>4.05	108	114		50	172	
Total bilirubin (mg/dL)	≦0.82	136	99	0.7088	82	153	0.4671
	>0.82	81	53		41	93	
ICGR15 (%)	≦16.7	125	98	0.2224	77	146	0.6246
	>16.7	92	54		46	100	
Child-Pugh	A	206	152	0.0034	115	243	0.008
	B	11	0		8	3	
Anatomical resection	Anatomical	172	110	0.1583	106	176	0.0028
	Nonanatomical	45	42		17	70	
AFP (ng/mL)	≦20	102	81	0.0461	52	131	<0.0001
	20< & ≦1000	64	51		30	85	
	>1000	51	20		41	30	
AFP-L3 (%)	≦15	143	112	0.1147	68	187	<0.0001
	>15	74	40		55	59	
PIVKA II (mAU/mL)	≦40	52	58	0.0001	22	88	<0.0001
	40< & ≦1000	74	60		33	101	
	>1000	91	34		68	57	
Number	Single	122	113	0.0009	68	167	<0.0001
	2, 3	60	29		27	62	
	≧4	35	10		28	17	
Size (cm)	≦3	48	68	<0.0001	15	101	<0.0001
	3< & ≦5	60	36		21	75	
	>5	109	48		87	70	
Differentiation	Well	12	8	0.0981	6	14	0.0003
	Moderately	102	88		46	144	
	Poorly	103	56		71	88	
vp	Positive	67	27	0.0065	49	45	<0.0001
	Negative	150	125		74	201	
vv	Positive	29	6	0.0043	24	11	<0.0001
	Negative	188	146		99	235	
Macroscopic vascular invasion	Positive	43	5	<0.0001	32	16	<0.0001
	Negative	174	147		91	230	
Stage	1	7	19	<0.0001	3	23	<0.0001
	2	88	84	45	127		
	3	71	40	35	76		
	4A	51	9	40	20		
Noncancerous liver	Cirrhosis	71	49	0.9876	35	85	0.2888
	Noncirrhosis	146	103		88	161	

AFP, alpha-fetoprotein; PIVKA-II, protein induced by vitamin K absence or antagonism factor II; AFP-L3, lens culinaris agglutinin-reactive fraction of alpha-fetoprotein; vp, microscopic tumor thrombus in the portal vein; vv, microscopic tumor thrombus in the hepatic vein; HBV, hepatitis B virus s antigen; HCV, anti-hepatitis C virus antibody; ICGR15, indocyanin green retention rate at 15 minutes.

chosen for further analysis. These selected molecules were assessed for any correlation with surgical outcomes in the HCC cohort (i.e., prognosis and recurrence) by univariate and multivariate analysis. G3560 *N*-glycan was found to be a significant prognostic factor and G2890 *N*-glycan was found to be a significant recurrence factor for this disease. Moreover, G2890 and G3560 were found to strongly correlate with a number of well-known tumor-related prognostic and recurrent factors. These results show that quantitative glycoblotting based on whole serum *N*-glycan profiling is a potent screening approach for novel HCC biomarkers, and that the G3560 and G2890 *N*-glycans are promising biomarkers of the PS, DFS, and malignant behavior characteristics of HCC after hepatectomy.

Although glycans, once released from glycoproteins or glycopeptides, have been subjected to fluorescent labeling and purification for detection by high-performance liquid chromatography (HPLC) previously, this method is time-consuming and therefore not suited to clinical diagnosis. Our novel analytical method, which we refer to as glycoblotting, is far more rapid and accurate, as evidenced by the number of *N*-glycans detected in our current analysis. This chemoselective glycan enrichment technology known as glycoblotting was developed in our laboratory to purify oligosaccharides derived from glycoproteins in an effective and quantitative manner, thus enabling serum glycan profiling by way of a simpler method.[20] Our method is also applicable to the fully automated analysis of multiple samples simultaneously. It readily combines the isolation and labeling of oligosaccharides, which can then be subjected to conventional analytical methods including MS. We had already achieved high-speed quantitative and qualitative profiling of glycan expression patterns in biological materials using this technology. In our present study, we improved the method to allow quantitative analysis of high reproducibility and accuracy using a calibration curve of human serum standards. The analysis of the obtained 67 glycan profiles was performed using this new developed technology. The effectiveness of our method is evidenced by the identification of the G2890 and G3560 *N*-glycans as highly promising clinical markers of HCC associated with the PS, DFS, and tumor malignancy rates of these cancers.

It has been reported that AFP is the most significant tumor marker and independent predictor of prognosis for HCC,[26] even in patients who have received a hepatectomy.[27] Although high levels of AFP in cases of fully developed HCC, or in the serum of the host, are known to be associated with more aggressive behavior, and increased anaplasis,[28] AFP can also cause apoptosis in tumor cells.[29] Moreover, it has been suggested that AFP regulates the immune response and induces either stimulatory or inhibitory growth activity.[30] On the other hand, it is well known that AFP may increase in some patients with acute and chronic hepatitis without HCC,[31,32] and that the elevation of AFP correlates with inflammation of background disease and hepatocyte regeneration.[33] Hence, because the AFP profile does not always directly reflect the extent of tumor malignancy, the AFP levels do not influence patient survival and recurrence. On the other hand, AFP and many important tumor markers, such as carcinoembryonic antigen, carbohydrate antigen 125, and carbohydrate antigen 19-9, are glycoproteins, and this means that the glycan profiles in serum are altered by the onset of cancer. Indeed, the profiling of serum glycans has been performed previously as a screen for distinct potential glycan biomarkers of ovarian cancer and breast cancer.[18,19] Hence, we surmised that highly specific glycoprotein markers of HCC should be detected by monitoring the serum glycosylation profile in these patients. In glycan structure, both G2890 and G3560 are multiply branched (G2890 is tri-antennary and G3560 is tetra-antennary) glycans with a core fucose. In addition, both glycans have one nonsialylated branch, i.e., G2890 and G3560, are tri-antennary di-sialylated glycan, and tetra-antennary tri-sialylated glycan, respectively. The structure of G2890 and G3560 is quite different from the AFC-L3 (core fucosylated bi-antennary glycan) and CA19-9 (sialylated Lewis (a) antigen), which are well-known biomarkers related to HCC except for the core fucosylation.

There have been several previous studies of glycans in HCC. Kudo et al.[34] reported that *N*-glycan alterations are associated with drug resistance in HCC *in vitro*. In other reported clinical studies, only specific glycans have been assessed in relation to HCC. Vanhooren et al.[17] were the first to analyze the function of HCC-specific glycans, and reported that a triantennary glycan (NA-3Fb) correlated with the tumor stage and AFP levels in HCC patients. However, that study analyzed 44 patients with HCC but did not evaluate the relationship between the *N*-glycans and the clinical and pathological factors of this disease, the clinical course after hepatectomy, or prognosis and recurrence. In our current study, in contrast, we analyzed a far larger cohort than any other previous report, and evaluated a comprehensive panel of clinical and pathological parameters in relation to the *N*-glycan profile in HCC. Tang et al.[35] also described some HCC-specific glycans in their previous study that we did not find to be significant in our current analyses. This is likely due to the fact that the patient number in their study was smaller than ours, and the fact that the *N*-glycome profile in serum is gender- and age-dependent.[36] In this study, the mean age and the distribution of gender and infection of hepatitis B and C virus were the difference between NC and HCC patients. However, the selected 14 serum *N*-glycans were quantified by our MALDI-TOF MS analysis and compared with NC by ROC analysis. These were statistically different between HCC and NC with respect to the quantity. Because these 14 serum *N*-glycans of which the AUC values were greater than 0.80 were revealed to be specific for HCC, they had a high discriminating ability to differentiate HCC from NC. Further analyses are

required to determine whether G2890 and G3560 are elevated in patients with hepatitis B, hepatitis C, and/or cirrhosis without HCC.

The most important adverse prognostic factor for liver resection and transplantation in HCC has been found to be microscopic venous invasion.[5] However, microscopic portal invasion is not diagnosed preoperatively, and is revealed only by pathological examination. New biomarkers that are more strongly associated with prognosis and recurrence of HCC than AFP, AFP-L3, or PIVKA-II are therefore highly desirable. Our current data show that the *N*-glycans G2890 and G3560 correlate closely with well-known tumor-related prognostic and recurrent factors such as tumor number, size, microscopic portal vein invasion, microscopic hepatic vein invasion, differentiation, macroscopic vascular invasion, stage, AFP, AFP-L3, and PIVKA-II (Table 6). Moreover, when G2890 and G3560 were simultaneously included in multivariate analysis for PS and DFS with AFP, AFPL3 and PIVKA-II, *P*-values of G2890 and G3560 were lower than AFP, and AFPL3, and PIVKA-II were not selected as valuables by AIC. We demonstrate that these are novel independent prognostic factors for HCC that are related to the survival and recurrence of this disease and that show a lower *P*-value than other established tumor factors. Hence, we predict that G2890 and G3560 will prove to be markers that can preoperatively predict HCC tumor malignancy including microscopic portal vein invasion, and the PS and DFS rates more accurately and with more potency than the more well-known biomarkers.

Acknowledgment: We thank the staff of the Gastroenterological Surgery I, Graduate School of Medicine, and Faculty of Advanced Life Science, Frontier Research Center for Post-Genome Science and Technology, Hokkaido University, and System Instruments Co. Ltd., Science & Technology Systems Inc., Bruker Daltonics K. K., for their kind cooperation during this study.

References

1. Farazi PA, DePinho RA. Hepatocellular carcinoma pathogenesis: from genes to environment. Nat Rev Cancer 2006;6:674-687.
2. Arii S, Yamaoka Y, Futagawa S, Inoue K, Kobayashi K, Kojiro M, et al. Results of surgical and nonsurgical treatment for small-sized hepatocellular carcinomas: a retrospective and nationwide survey in Japan. The Liver Cancer Study Group of Japan. HEPATOLOGY 2000;32:1224-1229.
3. Hasegawa K, Kokudo N, Imamura H, Matsuyama Y, Aoki T, Minagawa M, et al. Prognostic impact of anatomic resection for hepatocellular carcinoma. Ann Surg 2005;242:252-259.
4. Kamiyama T, Nakanishi K, Yokoo H, Kamachi H, Tahara M, Suzuki T, et al. Recurrence patterns after hepatectomy of hepatocellular carcinoma: implication of Milan criteria utilization. Ann Surg Oncol 2009;16:1560-1571.
5. Ikai I, Arii S, Kojiro M, Ichida T, Makuuchi M, Matsuyama Y, et al. Reevaluation of prognostic factors for survival after liver resection in patients with hepatocellular carcinoma in a Japanese nationwide survey. Cancer 2004;101:796-802.
6. Shah SA, Cleary SP, Wei AC, Yang I, Taylor BR, Hemming AW, et al. Recurrence after liver resection for hepatocellular carcinoma: risk factors, treatment, and outcomes. Surgery 2007;141:330-339.
7. Imamura H, Matsuyama Y, Miyagawa Y, Ishida K, Shimada R, Miyagawa S, et al. Prognostic significance of anatomical resection and des-gamma-carboxy prothrombin in patients with hepatocellular carcinoma. Br J Surg 1999;86:1032-1038.
8. Shimada M, Takenaka K, Fujiwara Y, Gion T, Kajiyama K, Maeda T, et al. Des-gamma-carboxy prothrombin and alpha-fetoprotein positive status as a new prognostic indicator after hepatic resection for hepatocellular carcinoma. Cancer 1996;78:2094-2100.
9. Shirabe K, Itoh S, Yoshizumi T, Soejima Y, Taketomi A, Aishima S, et al. The predictors of microvascular invasion in candidates for liver transplantation with hepatocellular carcinoma-with special reference to the serum levels of des-gamma-carboxy prothrombin. J Surg Oncol 2007;95:235-240.
10. Esnaola NF, Lauwers GY, Mirza NQ, Nagorney DM, Doherty D, Ikai I, et al. Predictors of microvascular invasion in patients with hepatocellular carcinoma who are candidates for orthotopic liver transplantation. J Gastrointest Surg 2002;6:224-232; discussion 232.
11. Tamura S, Kato T, Berho M, Misiakos EP, O'Brien C, Reddy KR, et al. Impact of histological grade of hepatocellular carcinoma on the outcome of liver transplantation. Arch Surg 2001;136:25-30; discussion 31.
12. Toyoda H, Kumada T, Kiriyama S, Sone Y, Tanikawa M, Hisanaga Y, et al. Prognostic significance of simultaneous measurement of three tumor markers in patients with hepatocellular carcinoma. Clin Gastroenterol Hepatol 2006;4:111-117.
13. Inoue S, Nakao A, Harada A, Nonami T, Takagi H. Clinical significance of abnormal prothrombin (DCP) in relation to postoperative survival and prognosis in patients with hepatocellular carcinoma. Am J Gastroenterol 1994;89:2222-2226.
14. Imamura H, Matsuyama Y, Tanaka E, Ohkubo T, Hasegawa K, Miyagawa S, et al. Risk factors contributing to early and late phase intrahepatic recurrence of hepatocellular carcinoma after hepatectomy. J Hepatol 2003;38:200-207.
15. Sumie S, Kuromatsu R, Okuda K, Ando E, Takata A, Fukushima N, et al. Microvascular invasion in patients with hepatocellular carcinoma and its predictable clinicopathological factors. Ann Surg Oncol 2008;15:1375-1382.
16. Kang P, Madera M Jr WRA, Goldman R, Mechref Y, Novotny MV. Glycomic alterations in the highly-abundant and lesser-abundant blood serum protein fractions for patients diagnosed with hepatocellular carcinoma. Int J Mass Spectrom 2011;305:185-198.
17. Vanhooren V, Liu XE, Franceschi C, Gao CF, Libert C, Contreras R, et al. N-glycan profiles as tools in diagnosis of hepatocellular carcinoma and prediction of healthy human ageing. Mech Ageing Dev 2009;130:92-97.
18. Kirmiz C, Li B, An HJ, Clowers BH, Chew HK, Lam KS, et al. A serum glycomics approach to breast cancer biomarkers. Mol Cell Proteomics 2007;6:43-55.
19. An HJ, Miyamoto S, Lancaster KS, Kirmiz C, Li B, Lam KS, et al. Profiling of glycans in serum for the discovery of potential biomarkers for ovarian cancer. J Proteome Res 2006;5:1626-1635.
20. Miura Y, Hato M, Shinohara Y, Kuramoto H, Furukawa J, Kurogochi M, et al. BlotGlycoABCTM, an integrated glycoblotting technique for rapid and large scale clinical glycomics. Mol Cell Proteomics 2008;7:370-377.
21. Nishimura S, Niikura K, Kurogochi M, Matsushita T, Fumoto M, Hinou H, et al. High-throughput protein glycomics: combined use of

chemoselective glycoblotting and MALDI-TOF/TOF mass spectrometry. Angew Chem Int Ed Engl 2004;44:91-96.
22. Furukawa J, Shinohara Y, Kuramoto H, Miura Y, Shimaoka H, Kurogochi M, et al. Comprehensive approach to structural and functional glycomics based on chemoselective glycoblotting and sequential tag conversion. Anal Chem 2008;80:1094-1101.
23. Ichida F, Tsuji T, Omata M, Ichida T, Inoue K, Kamimura T, et al. New Inuyama Classification; new criteria for histlogical assessment of chronic hepatitis. Int Hepatol Commun 1996;6:112-119.
24. The Liver Study Group of Japan. The general rules for the clinical and pathological study of primary liver cancer. 3rd English ed. Tokyo, Japan: Kanehara & Co.
25. Akaike H. A new look at the statistical model identification. IEEE Trans Autom Control 1974;19:716-723.
26. Nomura F, Ohnishi K, Tanabe Y. Clinical features and prognosis of hepatocellular carcinoma with reference to serum alpha-fetoprotein levels. Analysis of 606 patients. Cancer 1989;64:1700-1707.
27. Hanazaki K, Kajikawa S, Koide N, Adachi W, Amano J. Prognostic factors after hepatic resection for hepatocellular carcinoma with hepatitis C viral infection: univariate and multivariate analysis. Am J Gastroenterol 2001;96:1243-1250.
28. Matsumoto Y, Suzuki T, Asada I, Ozawa K, Tobe T, Honjo I. Clinical classification of hepatoma in Japan according to serial changes in serum alpha-fetoprotein levels. Cancer 1982;49:354-360.
29. Yang X, Zhang Y, Zhang L, Mao J. Silencing alpha-fetoprotein expression induces growth arrest and apoptosis in human hepatocellular cancer cell. Cancer Lett 2008;271:281-293.
30. Mizejewski GJ. Alpha-fetoprotein structure and function: relevance to isoforms, epitopes, and conformational variants. Exp Biol Med (Maywood) 2001;226:377-408.
31. Smith JB. Occurrence of alpha-fetoprotein in acute viral hepatitis. Int J Cancer 1971;8:421-424.
32. Silver HK, Gold P, Shuster J, Javitt NB, Freedman SO, Finlayson ND. Alpha(1)-fetoprotein in chronic liver disease. N Engl J Med 1974;291:506-508.
33. Fujiyama S, Tanaka M, Maeda S, Ashihara H, Hirata R, Tomita K. Tumor markers in early diagnosis, follow-up and management of patients with hepatocellular carcinoma. Oncology 2002;62(Suppl 1):57-63.
34. Kudo T, Nakagawa H, Takahashi M, Hamaguchi J, Kamiyama N, Yokoo H, et al. N-glycan alterations are associated with drug resistance in human hepatocellular carcinoma. Mol Cancer 2007;6:32.
35. Tang Z, Varghese RS, Bekesova S, Loffredo CA, Hamid MA, Kyselova Z, et al. Identification of N-glycan serum markers associated with hepatocellular carcinoma from mass spectrometry data. J Proteome Res 2010;9:104-112.
36. Ding N, Nie H, Sun X, Sun W, Qu Y, Liu X, et al. Human serum N-glycan profiles are age and sex dependent. Age Ageing 2011;40:568-575.

miR-1290 and its potential targets are associated with characteristics of estrogen receptor α-positive breast cancer

Yumi Endo[1], Tatsuya Toyama[1], Satoru Takahashi[2], Nobuyasu Yoshimoto[1], Mai Iwasa[1], Tomoko Asano[1], Yoshitaka Fujii[1] and Hiroko Yamashita[1]

Departments of [1]Oncology, Immunology and Surgery [2]Experimental Pathology and Tumor Biology, Nagoya City University Graduate School of Medical Sciences, 1 Kawasumi, Mizuho-cho, Mizuho-ku, Nagoya 467-8601, Japan

H Yamashita is now at Breast and Endocrine Surgery, Hokkaido University Hospital, Kita 14, Nishi 5, Sapporo 060-8648, Japan

Correspondence should be addressed to H Yamashita
Email
hirokoy@huhp.hokudai.ac.jp

Abstract

Recent analyses have identified heterogeneity in estrogen receptor α (ERα)-positive breast cancer. Subtypes called luminal A and luminal B have been identified, and the tumor characteristics, such as response to endocrine therapy and prognosis, are different in these subtypes. However, little is known about how the biological characteristics of ER-positive breast cancer are determined. In this study, expression profiles of microRNAs (miRNAs) and mRNAs in ER-positive breast cancer tissue were compared between ER^{high} $Ki67^{low}$ tumors and ER^{low} $Ki67^{high}$ tumors by miRNA and mRNA microarrays. Unsupervised hierarchical clustering analyses revealed distinct expression patterns of miRNAs and mRNAs in these groups. We identified a downregulation of miR-1290 in ER^{high} $Ki67^{low}$ tumors. Among 11 miRNAs that were upregulated in ER^{high} $Ki67^{low}$ tumors, quantitative RT-PCR detection analysis using 64 samples of frozen breast cancer tissue identified six miRNAs (let-7a, miR-15a, miR-26a, miR-34a, miR-193b, and miR-342-3p). We picked up 11 genes that were potential target genes of the selected miRNAs and that were differentially expressed in ER^{high} $Ki67^{low}$ tumors and ER^{low} $Ki67^{high}$ tumors. Protein expression patterns of the selected target genes were analyzed in 256 ER-positive breast cancer samples by immunohistochemistry: miR-1290 and its putative targets, *BCL2, FOXA1, MAPT,* and *NAT1*, were identified. Transfection experiments revealed that introduction of miR-1290 into ER-positive breast cancer cells decreased expression of NAT1 and FOXA1. Our results suggest that miR-1290 and its potential targets might be associated with characteristics of ER-positive breast cancer.

Key Words
- breast cancer
- microRNA
- estrogen receptor
- miR-1290

Endocrine-Related Cancer (2013) **20**, 91–102

Introduction

There are large-scale molecular differences between estrogen receptor α (ERα)-positive and ER-negative breast cancers (Sorlie *et al.* 2003). ER is essential for estrogen-dependent growth, and its level of expression is a crucial determinant of response to endocrine therapy and prognosis in ER-positive breast cancer (Harvey *et al.* 1999, Yamashita *et al.* 2006, Dowsett *et al.* 2008). Recent analyses have identified heterogeneity in ER-positive

http://erc.endocrinology-journals.org
DOI: 10.1530/ERC-12-0207

Published by Bioscientifica Ltd.

breast cancer. Subtypes, named luminal A and luminal B, have been defined according to expression levels of Ki67, and the characteristics of these two subtypes are different (Goldhirsch *et al.* 2011). There is no doubt that higher concentrations of ER in the tumor cells are associated with a greater likelihood of a favorable response to endocrine therapy. However, little is known about how the expression of ER in breast cancer cells is regulated and how the biological characteristics of ER-positive breast cancer are determined. We recently analyzed expressions of microRNAs (miRNAs) that directly target ER in breast cancer. We found that miR-206 and miR-18a were downregulated in ER-positive breast cancer compared with ER-negative tumors and that low miR-18b expression was significantly associated with improved survival in HER2-negative breast cancer, although miR-18b expression was not correlated with ER protein expression (Kondo *et al.* 2008, Yoshimoto *et al.* 2011).

miRNAs are small (~21 nucleotides) noncoding RNAs that negatively regulate target genes by predominantly binding to the 3′-untranslated region (3′-UTR) of target mRNA, resulting in either mRNA degradation or translational repression (Krol *et al.* 2010). Recent studies have shown that miRNA mutations or dysregulated expression were associated with various human cancers and indicated that miRNAs can function as tumor suppressor genes and oncogenes (Esquela-Kerscher & Slack 2006). Expression profiling also revealed that miRNAs are differently expressed among molecular subtypes of breast cancer (Iorio *et al.* 2005). Significant associations were found between miRNA expression profiles and clinicopathological factors such as ER status and tumor grade (Blenkiron *et al.* 2007). Furthermore, recent studies have demonstrated that loss- or gain-of-function of specific miRNAs contributes to breast epithelial cellular transformation, tumorigenesis, and epithelial–mesenchymal transition and metastasis (Zhang & Ma 2012).

In this study, expression profiles of miRNAs and mRNAs in ER-positive breast cancer tissue were compared between ER^{high} $Ki67^{low}$ tumors and ER^{low} $Ki67^{high}$ tumors by miRNA and mRNA microarrays. Unsupervised hierarchical clustering analyses revealed distinct expression patterns of miRNAs and mRNAs in these two groups. We demonstrated that miR-1290 was downregulated and that six miRNAs were upregulated in ER^{high} $Ki67^{low}$ tumors. Protein expression patterns of the predicted target genes and the genes that were identified by mRNA expression profiling were analyzed in ER-positive breast cancer samples by immunohistochemistry (IHC). We identified miR-1290 and its potential target genes, forkhead box A1 (*FOXA1*) and *N*-acetyltransferase-1 (*NAT1*), being associated with characteristics of ER-positive breast cancer.

Materials and methods

Patients and breast cancer tissue

Breast tumor specimens from female patients with invasive breast carcinoma who were treated at Nagoya City University Hospital between 1995 and 2010 were included in the study (Table 1). The study protocol was approved by the institutional review board and conformed to the guidelines of the 1996 Declaration of Helsinki. Written informed consent for the use of surgically resected tumor tissues was provided by all patients before treatments. The samples were chosen from a continuous series of invasive carcinoma. All patients except those with stage IV disease underwent surgical treatment (mastectomy or lumpectomy). Tumor samples of patients with stage IV disease were taken by core needle biopsy. Patients received adequate endocrine or chemotherapy for adjuvant or metastatic diseases.

Microarray profiling of miRNA and mRNA expression

Total RNA was extracted from eight frozen samples of breast cancer tissue (Table 1). Extracted total RNA was labeled with Hy5 using the miRCURY LNA Array miR labeling kit (Exiqon, Vedbaek, Denmark). Labeled RNAs were hybridized onto 3D-Gene Human miRNA Oligo chips containing 1011 antisense probes printed in duplicate spots (Toray, Kamakura, Japan). The annotation and oligonucleotide sequences of the probes were conformed to the miRBase miRNA data base (http://microrna.sanger.ac.uk/sequences/). After stringent washes, fluorescent signals were scanned with the ScanArray Express Scanner (PerkinElmer, Waltham, MA, USA) and analyzed using GenePix Pro version 5.0 (Molecular Devices, Sunnyvale, CA, USA). These raw data of each spot were normalized by substitution with the mean intensity of the background signal determined by all blank spots' signal intensities at 95% confidence intervals. Measurements of both duplicate spots with signal intensities >2 S.D. of the background signal intensity were considered to be valid. A relative expression level of a given miRNA was calculated by comparing the signal intensities of the averaged valid spots with their mean value throughout the microarray experiments after normalization by their median values adjusted equivalently. miRNAs differentially expressed

http://erc.endocrinology-journals.org
DOI: 10.1530/ERC-12-0207

Published by Bioscientifica Ltd.

among the ER^{high} $Ki67^{low}$ tumors and ER^{low} $Ki67^{high}$ tumors were statistically identified using the Student's *t*-test and unsupervised hierarchical clustering analyses. Hierarchical clustering was performed with average linkage and Pearson's correlation. Differential expression was assessed by a nonparametric Wilcoxon's rank sum test for comparison between two groups. A heat-map was constructed by hierarchical clustering analysis using Cluster 2.0 Software (Tokyo, Japan) and the results were displayed with the TreeView program (http://rana.lbl.gov/eisen/). miRNA expression data are available from the National Center for Biotechnology Gene Expression Omnibus (GEO) at accession number (GEO:GSE38280).

mRNA expression profiles were examined using the same frozen breast cancer tissue samples as those used in miRNA analyses. Extracted total RNA was labeled with Cy5 using the Amino Allyl MessageAMP II aRNA Amplification kit (Applied Biosystems). Labeled RNAs were hybridized onto 3D-Gene Human mRNA Oligo chips 25k (Toray) was used (25 370 distinct genes). Hybridization signals were scanned and detected by the same method as that used in miRNA analyses. The gene expression data are available from GEO at accession number (GEO:GSE38280).

Quantitative RT-PCR detection of miRNAs

Total RNA was extracted from ~500 mg frozen breast cancer tissue using TRIzol reagent (Life Technologies, Inc.) as described previously (Kondo *et al.* 2008). cDNA was reverse transcribed from total RNA samples using specific miRNA primers from the TaqMan MicroRNA Assays and reagents from the TaqMan MicroRNA RT Kit (Applied Biosystems). The resulting cDNA was amplified by PCR using TaqMan MicroRNA Assay primers with the TaqMan Universal PCR Master Mix and analyzed with a 7300 ABI PRISM Sequence Detector System according to the manufacturer's instructions (Applied Biosystems). The relative levels of miRNA expression were calculated from the relevant signals by normalization with the signal for *U6B* miRNA expression. The assay names for each miRNA were as follows: hsa-let-7a for let-7a, hsa-miR-10a for miR-10a, hsa-miR-10b for miR-10b, hsa-miR-15a for 15a, hsa-miR-18a for miR-18a, hsa-miR-26a for miR-26a, hsa-miR-29c for miR-29c, hsa-miR-34a for miR-34a, hsa-miR-129 for miR-129, hsa-miR-146a for miR-146a, hsa-miR-193b for miR-193b, hsa-miR-342-3p for miR-342-3p, hsa-miR-1290 for miR-1290, and RNU6B for U6B miRNA (Applied Biosystems).

Immunohistochemistry

Tissue microarrays were constructed using paraffin-embedded, formalin-fixed tissue from 256 ER-positive breast cancer samples, including 64 samples from patients whose frozen samples were used in miRNA expression analysis. Tissue array sections were immunostained with 15 commercially available antibodies using the Bond-Max Autostainer (Leica Microsystems, Newcastle, UK) and the associated Bond Refine Polymer Detection Kit (Yamashita *et al.* 2006). Details of primary antibodies and scoring manners are described in Supplementary Table 1, see section on supplementary data given at the end of this article. HER2-positive tumors were excluded from this study.

Cell culture and transfections

MCF-7 cells (American Type Culture Collection (ATCC), Manassas, VA, USA) were grown in RPMI 1640 medium containing 10% fetal bovine serum (FBS), 2 mmol/l L-glutamine and penicillin–streptomycin (50 IU/ml and 50 mg/ml respectively), and 0.1% human insulin at 37 °C with 5% CO_2. T47D cells (ATCC) were grown in RPMI 1640 medium containing 10% FBS and 2 mmol/l L-glutamine and penicillin–streptomycin (50 IU/ml and 50 mg/ml respectively) at 37 °C with 5% CO_2. Transfections of pre-miR-1290 precursor (hsa-miR-1290; Ambion, Inc., Austin, TX, USA) were performed with Cell Line Nucleofector kits (Amaxa Biosystems, Cologne, Germany) using a Nucleofector device (Amaxa Biosystems) according to the manufacturer's instructions (Kondo *et al.* 2008). A nonspecific control miRNA (Pre-miR miRNA Inhibitors-Negative Control #1; Ambion, Inc.) was used as a negative control.

Quantitative RT-PCR detection of miR-1290 and mRNAs

Total RNA was extracted from 2×10^6 cells with miRNeasy Mini Kit (Qiagen) using a QIAcube (Qiagen) according to the manufacturer's instructions. cDNA was reverse transcribed using specific miRNA primers and the relative levels of miR-1290 expression were measured as described earlier. Total RNA (1 μg) was also subjected to RT with random primers in a 20 μl reaction volume using High-Capacity cDNA RT Kit (Applied Biosystems). mRNA expression was measured by quantitative RT-PCR with the TaqMan Universal PCR Master Mix using a 7500 ABI PRISM Sequence Detector System according to the manufacturer's instructions (Applied Biosystems; Kondo *et al.* 2008). The relative levels of mRNA expression were

http://erc.endocrinology-journals.org
DOI: 10.1530/ERC-12-0207

Published by Bioscientifica Ltd.

Table 1 Clinicopathological characteristics of patients and breast tumors with ER-positive, HER2-negative breast cancer.

	Samples for miRNA and mRNA microarray analyses		Samples for miRNA quantitative RT-PCR analysis	Samples for immunohistochemistry
	ER^{high} $Ki67^{low}$	ER^{low} $Ki67^{high}$	Total	Total
No. of patients	4	4	64	256
Age (years)				
Mean±S.D.	71.8±20.9	57.5±12.1	60.0±12.0	58.0±13.0
Range	44–91	42–69	32–88	28–91
Tumor size (cm)				
Mean±S.D.	1.5±0.4	1.6±0.7		
≤2.0			20 (31%)	148 (57.9%)
2.1–5.0			38 (59%)	102 (39.8%)
>5.0			6 (10%)	6 (2.3%)
No. of positive lymph nodes				
0	4 (100%)	4 (100%)	34 (53%)	135 (52.7%)
1–3	0 (0%)	0 (0%)	16 (25%)	72 (28.1%)
4–9	0 (0%)	0 (0%)	6 (10%)	11 (4.3%)
≥10	0 (0%)	0 (0%)	4 (6%)	7 (2.7%)
Unknown	0 (0%)	0 (0%)	4 (6%)	31 (12.2%)
Tumor grade				
1	4 (100%)	0 (0%)	16 (25%)	95 (37.1%)
2	0 (0%)	0 (0%)	36 (56%)	69 (27.0%)
3	0 (0%)	4 (100%)	12 (19%)	92 (35.9%)
ER (Allred score)				
Mean±S.D.	7.8±0.5	3.5±0.6		
0–2 (negative)			0 (0%)	0 (0%)
3–8 (positive)			64 (100%)	256 (100%)
PgR (Allred score)				
Mean±S.D.	7.8±0.5	2.5±0.6		
0–2 (negative)			10 (16%)	34 (13.3%)
3–8 (positive)			54 (84%)	222 (86.7%)
HER2 status				
Negative	4 (100%)	4 (100%)	64 (100%)	256 (100%)
Positive	0 (0%)	0 (0%)	0 (0%)	0 (0%)
Ki67 (labeling index, %)				
Mean±S.D.	6.1±2.7	50.8±11.8		
Adjuvant therapy				
None			8	27
Endocrine therapy			32	127
Chemotherapy			3	4
Combined			21	98

calculated from the relevant signals by normalization with the signal for β-actin mRNA expression. The assay numbers for BCL2, FOXA1, microtubule-associated protein tau (MAPT), NAT1, and β-actin were as follows: Hs00608023_m1 for BCL2, Hs00270129_m1 for FOXA1, Hs00902314_m1 for MAPT, Hs00265080_m1 for NAT1, and 4333762T for β-actin (Applied Biosystems).

Western blotting

Cells were pelleted by centrifugation and solubilized in lysis buffer containing protease inhibitor and phosphatase inhibitor cocktails (Thermo Scientific, Yokohama, Japan). Equal amounts of total protein (30 μg) from whole cell lysates were prepared and electrophoresed on 12% (w/v) SDS–polyacrylamide gels (NuPAGE Bis–Tris Gel, Invitrogen) transferred to polyvinylidene difluoride membranes (Invitrogen) and immunoblotted using specific antibodies (Supplementary Table 1; Yamashita *et al.* 2003). Anti-mouse or anti-rabbit IgG, HRP-linked Whole Antibodies (GE Healthcare Japan, Tokyo, Japan) were used as secondary antibodies at 1:10 000 dilution. Antibody binding was visualized with ECL Western Blotting Detection System (GE Healthcare Japan) using Light-Capture AE-6981 (ATTO, Tokyo, Japan) according to the manufacturer's instructions. Image J Software from the National Institutes of Health (Bethesda, MD, USA) was used to quantify band intensities.

http://erc.endocrinology-journals.org
DOI: 10.1530/ERC-12-0207

Published by Bioscientifica Ltd.

Statistical analysis

Spearman's rank correlation test was used to study relationships between expression levels of miRNAs and clinicopathological factors, expression levels of proteins and clinicopathological factors, expression levels of miRNAs and proteins, and expression levels of miRNAs and mRNAs. $P<0.05$ is considered significant in Spearman's rank correlation test.

Results

Differentially expressed miRNAs in ER^{high} $Ki67^{low}$ tumors and ER^{low} $Ki67^{high}$ tumors in breast cancer tissue

Expression profiles of miRNAs and mRNAs in ER-positive breast cancer tissue were compared between ER^{high} $Ki67^{low}$ tumors and ER^{low} $Ki67^{high}$ tumors by miRNA and mRNA microarrays using eight frozen samples of breast cancer tissue (four tumors in each group; Table 1). Unsupervised hierarchical clustering analyses revealed 67 miRNAs in 1011 miRNAs and 657 mRNAs in 25 370 mRNAs that were differentially expressed in ER^{high} $Ki67^{low}$ tumors and ER^{low} $Ki67^{high}$ tumors ($P<0.01$; Supplementary Figure 1, see section on supplementary data given at the end of this article and Supplementary Table 2, see section on supplementary data given at the end of this article, and $P<0.01$; Supplementary Figure 2, see section on supplementary data given at the end of this article and Supplementary Tables 3 and 4, see section on supplementary data given at the end of this article respectively). We selected 12 miRNAs (let-7a, miR-10a, miR-10b, miR-15a, miR-26a, miR-29c, miR-34a, miR-129, miR-146a, miR-193b, miR-342-3p, and miR-1290) that were differentially expressed in these two groups. Among differentially expressed 67 miRNAs, the above 12 miRNAs, especially let-7a, miR-10a, miR-10b, miR-15a, miR-26a, miR-29c, miR-34a, miR-146a, and miR-342-3p, have been reported to be related to breast cancer development and carcinogenesis (Mattie *et al.* 2006, Blenkiron *et al.* 2007, O'Day & Lal 2010). miR-193b has been reported to be related to ERα (Yoshimoto *et al.* 2011). Moreover, we referred to the reported mRNA microarray analyses to classify luminal A and luminal B subtypes in order to select key genes (Sorlie *et al.* 2003, Parker *et al.* 2009), including *FOXA1*, *NAT1*, *MAPT*, *XBP1*, and *BCL2*, which have target sequences in the 3′-UTR regions of 67 differentially expressed miRNAs according to *in silico* analysis using TargetScan, PicTar, and MiRanda, and selected miR-146a and miR-1290, which were downregulated in ER^{high} $Ki67^{low}$ tumors. Quantitative RT-PCR detection analysis using 64 frozen breast cancer tissue samples (Table 2 and Supplementary Table 5, see section on supplementary data given at the end of this article) identified six miRNAs (let-7a, miR-15a, miR-26a, miR-34a, miR-193b, and miR-342-3p) that were upregulated in ER^{high} tumors ($P=0.0002$, $P=0.0006$, $P=0.0082$, $P<0.0001$, $P=0.0142$, and $P=0.0002$ respectively; Table 3). miR-1290 was also included in further analyses because it was the only miRNA among the selected miRNAs that was downregulated in ER^{high} $Ki67^{low}$ tumors and its expression levels were strongly correlated with tumor grade ($P<0.0001$; Table 3).

Table 2 Expression levels of 12 selected miRNAs and the control miRNA (U6B) in 64 ER-positive breast cancer tissues by quantitative RT-PCR analysis.

	Mean ± S.E.M.
let-7a	22.079 ± 0.173
miR-10a	26.585 ± 0.278
miR-10b	27.636 ± 0.247
miR-15a	27.100 ± 0.285
miR-26a	22.711 ± 0.201
miR-29c	24.295 ± 0.390
miR-34a	26.339 ± 0.240
mR-129	34.759 ± 0.185
miR-146a	26.160 ± 0.221
miR-193b	21.112 ± 0.219
miR-342-3p	24.456 ± 0.322
miR-1290	27.612 ± 0.445
U6B	27.091 ± 0.154

The potential target genes for seven selected miRNAs (let-7a, miR-15a, miR-26a, miR-34a, miR-193b, miR-342-3p, and miR-1290) were predicted according to *in silico* analysis using TargetScan, PicTar, and MiRanda. In addition, 657 mRNAs that were differentially expressed in ER^{high} $Ki67^{low}$ tumors and ER^{low} $Ki67^{high}$ tumors in microarray analysis were considered to select putative target genes. Finally, we picked up 11 proteins (ANKRD30, BCL2, cyclin D1, FOXA1, GATA3, LIN28, MAPT, NAT1, RB1, P53 (TP53), and XBP1) that were products of potential target genes for seven selected miRNAs and that were considered to be differentially expressed in ER^{high} $Ki67^{low}$ tumors and ER^{low} $Ki67^{high}$ tumors (Table 4). *ANKRD30* was the most differentially expressed gene between ER^{high} $Ki67^{low}$ tumors and ER^{low} $Ki67^{high}$ tumors. BCL2, cyclin D1, LIN28, and RB1 are potential targets of the selected miRNAs as shown in Table 4. FOXA1, GATA3, NAT1, and XBP1 were strongly downregulated in ER^{low} $Ki67^{high}$ tumors, putative targets of the selected miRNAs, and reported as to be related with ER-positive breast

http://erc.endocrinology-journals.org
DOI: 10.1530/ERC-12-0207

Published by Bioscientifica Ltd.

Table 3 Correlation between expression levels of miRNAs and clinicopathological factors ($n=64$).

	ER	PgR	Tumor grade	Ki67	Tumor size	No. of positive lymph nodes
let-7a	+0.533[a] 0.0002*[,b]	+0.349 0.0087*	−0.033 0.2536	−0.115 0.3717	−0.068 0.5854	+0.123 0.7959
miR-10a	+0.286 0.1114	+0.219 0.1113	+0.005 0.4012	−0.113 0.3757	−0.326 0.0098*	+0.132 0.7399
miR-10b	+0.268 0.1646	+0.130 0.3894	+0.074 0.8411	−0.114 0.375	−0.185 0.1439	+0.171 0.5025
miR-15a	+0.499 0.0006*	+0.081 0.6396	+0.215 0.3036	+0.055 0.6729	−0.129 0.3084	+0.062 0.7917
miR-26a	+0.414 0.0082*	+0.165 0.2585	+0.065 0.7953	−0.056 0.6674	−0.003 0.9712	+0.060 0.8038
miR-29c	+0.206 0.3839	−0.030 0.6671	+0.115 0.8782	+0.018 0.8917	−0.084 0.5117	+0.121 0.7546
miR-34a	+0.785 <0.0001*	+0.164 0.2558	+0.061 0.7535	+0.034 0.7941	−0.168 0.1851	+0.039 0.6458
mR-129	+0.334 0.0528	+0.043 0.8722	+0.334 0.0384*	−0.056 0.6711	−0.006 0.9746	+0.049 0.677
miR-146a	+0.101 0.9032	−0.149 0.1819	+0.425 0.0073*	+0.007 0.9586	−0.052 0.6966	−0.009 0.5031
miR-193b	+0.387 0.0142*	+0.203 0.1483	+0.223 0.2666	+0.078 0.5493	+0.046 0.7298	+0.214 0.2889
miR-342-3p	+0.539 0.0002*	+0.131 0.3975	+0.131 0.8024	−0.039 0.7657	−0.016 0.8932	+0.107 0.9081
miR-1290	+0.014 0.3987	−0.211 0.0581	+0.585 <0.0001*	+0.228 0.0748	+0.029 0.8267	+0.280 0.1109

*$P<0.05$ is considered significant.
[a]Spearman's correlation coefficient.
[b]P, Spearman's rank correlation test.

cancer. MAPT is also reported to be related with ER-positive breast cancer and a potential target of miR-1290. P53 was selected as a target of let-7a.

Expression of the potential target genes in ER-positive, HER2-negative breast cancer

We examined protein expression of 11 selected target genes in ER-positive, HER2-negative breast cancer by IHC (Supplementary Table 6, see section on supplementary data given at the end of this article). Expression levels of BCL2, FOXA1, GATA3, LIN28, MAPT, and NAT1 were positively correlated with expression levels of ER ($P<0.0001$, $P<0.0001$, $P<0.0001$, $P=0.0008$, $P<0.0001$, and $P=0.0005$ respectively; Table 4). Expression levels of ANKRD30, BCL2, FOXA1, GATA3, LIN28, MAPT, and NAT1 were positively correlated with expression levels of progesterone receptor (PgR; $P=0.0246$, $P=0.0059$, $P=0.0005$, $P<0.0001$, $P=0.017$, $P<0.0001$, and $P<0.0001$ respectively). Expression levels of ANKRD30, BCL2, and TP53 were positively correlated with tumor grade ($P=0.0012$, $P=0.0109$, and $P=0.0108$ respectively), whereas expression levels of CCND1, FOXA1, GATA3, LIN28, MAPT, NAT1, and XBP1 were negatively correlated with tumor grade ($P=0.0101$, $P<0.0001$, $P<0.0001$, $P=0.0099$, $P<0.0001$, $P<0.0001$, and $P=0.0018$ respectively). Expression levels of LIN28 and TP53 were positively correlated with expression levels of Ki67 ($P=0.0446$ and $P=0.002$ respectively), while expression levels of MAPT and NAT1 were negatively correlated with expression levels of Ki67 ($P=0.0419$ and $P=0.0095$ respectively). Expression levels of ANKRD30, FOXA1, GATA3, LIN28, MAPT, NAT1, TP53, and XBP1 were negatively correlated with tumor size ($P<0.0001$, $P=0.0009$, $P=0.0001$, $P<0.0001$, $P=0.0093$, $P=0.0004$, $P=0.0336$, and $P=0.0203$ respectively). There was no association between expression of 11 selected proteins and lymph node status (Table 4).

We then compared expression levels of seven selected miRNAs (let-7a, miR-15a, miR-26a, miR-34a, miR-193b, miR-342-3p, and miR-1290) and their potential target genes (*ANKRD30*, *BCL2*, cyclin D1, *FOXA1*, *GATA3*, *LIN28*, *MAPT*, *NAT1*, *RB1*, *P53*, and *XBP1*) using 64 samples of breast cancer tissue, simultaneously analyzing miRNA expression by quantitative RT-PCR and protein expression by IHC. Interestingly, expression levels of miR-1290 were

http://erc.endocrinology-journals.org
DOI: 10.1530/ERC-12-0207

Published by Bioscientifica Ltd.

Table 4 Correlation between expression levels of potential target proteins and clinicopathological factors ($n=256$).

	ER	PgR	Tumor grade	Ki67	Tumor size	No. of positive lymph nodes	miRNAs
ANKRD30	+0.260[a] 0.2265[b]	+0.250 0.0246*	+0.002 0.0012*	+0.142 0.5865	−0.145 <0.0001*	+0.176 0.2769	miR-193b
BCL2	+0.467 <0.0001*	+0.320 0.0059*	+0.102 0.0109*	+0.132 0.4585	+0.078 0.0968	+0.278 0.8608	let-7a, miR-10a, miR-15a, miR-26a, miR-29c, miR-34a, miR-1290
CCND1	+0.177 0.5364	+0.083 0.6216	−0.190 0.0101*	+0.078 0.5415	−0.085 0.4981	+0.046 0.6898	miR-15a, miR-34a, miR-193b
FOXA1	+0.407 <0.0001*	+0.234 0.0005*	−0.235 <0.0001*	−0.082 0.1939	−0.210 0.0009*	+0.009 0.103	miR-129, miR-1290
GATA3	+0.448 <0.0001*	+0.286 <0.0001*	−0.224 <0.0001*	−0.004 0.9441	−0.242 0.0001*	−0.005 0.0655	miR-10a, miR-10b, miR-34a
LIN28	+0.289 0.0008*	+0.173 0.017*	−0.081 0.0099*	+0.138 0.0446*	−0.238 <0.0001*	+0.068 0.3681	let-7a, miR-26a, miR-34a, miR-129, miR-342-3p
MAPT	+0.356 <0.0001*	0.494 <0.0001*	−0.254 <0.0001*	−0.144 0.0419*	−0.149 0.0093*	+0.030 0.1314	miR-34a, miR-1290
NAT1	+0.316 0.0005*	+0.394 <0.0001*	−0.274 <0.0001*	−0.122 0.0095*	−0.180 0.0004*	+0.105 0.4956	miR-1290
RB1	+0.248 0.0751	+0.261 0.8369	+0.327 0.4651	+0.290 0.2424	+0.263 0.6956	+0.374 0.6748	let-7a, miR-26a, miR-34a, miR-129, miR-1290
TP53	−0.016 0.0743	−0.010 0.6815	+0.211 0.0108*	+0.197 0.002*	−0.133 0.0336*	+0.074 0.5783	let-7a
XBP1	+0.183 0.5653	−0.042 0.5318	−0.236 0.0018*	+0.079 0.5906	−0.278 0.0203*	−0.040 0.2069	miR-34a

*$P<0.05$ is considered significant.
[a]Spearman's correlation coefficient.
[b]P, Spearman's rank correlation test.

inversely correlated with expression levels of *BCL2*, *FOXA1*, *MAPT*, and *NAT1*, all of which are predictive targets of miR-1290 according to *in silico* analysis ($P=0.020$, $P=0.044$, $P=0.040$, and $P=0.0098$ respectively; Fig. 1A, B, C and D), suggesting that miR-1290 might downregulate these four genes in ER-positive breast cancer. Moreover, let-7a expression was inversely correlated with P53 expression ($P=0.038$; Fig. 1E). No association was found between other miRNA expressions and their putative target gene expressions.

miR-1290 downregulates FOXA1 and NAT1 in ER-positive breast cancer cells

We extended our analysis to clarify whether miR-1290 downregulates BCL2, FOXA1, MAPT, and NAT1 in ER-positive breast cancer cells. Pre-miR-1290 precursor was introduced into T47D and MCF-7 cells. Cells were transfected with either control miRNA (300 nmol/l) or pre-miR-1290 precursor at various concentrations (10–300 nmol/l) and incubated for 24 h in T47D cells and for 36 h in MCF-7 cells. Expression levels of miR-1290 and mRNA expression levels of *BCL2*, *FOXA1*, *MAPT*, and *NAT1* were quantitatively measured using parallel samples. Transfection with pre-miR-1290 produced a dose-dependent increase in miR-1290 expression levels (Fig. 2A, left), whereas expression levels of miR-1290 were inversely correlated with expression levels of *FOXA1* ($P=0.0003$; Fig. 2A, top right) and *NAT1* ($P<0.0001$; Fig. 2A, bottom right) mRNAs, but not with *BCL2* or *MAPT* mRNA, in T47D cells (Fig. 2A). Moreover, expression levels of miR-1290 were inversely correlated with expression levels of *NAT1* mRNA ($P=0.037$; Fig. 2B, bottom right), but not with *BCL2*, *FOXA1*, or *MAPT* mRNA, in MCF-7 cells (Fig. 2B).

The effects of miR-1290 on protein expression of BCL2, FOXA1, MAPT, and NAT1 were examined in T47D and MCF-7 cells by western blot analysis. When T47D cells were transfected with either control miRNA (300 nmol/l) or pre-miR-1290 precursor at various concentrations (30–1000 nmol/l) and incubated for 48 h, miR-1290 induced a dose-dependent decrease in protein expression of NAT1, reducing it ~60%, but not BCL2, FOXA1, or MAPT (Fig. 2C). Effects of miR-1290 on protein expression of BCL2, FOXA1, MAPT, and NAT1 were not clear in MCF-7 cells (Fig. 2D). From these analyses, we conclude that miR-1290 might downregulate FOXA1 and NAT1 in ER-positive breast cancer cells.

http://erc.endocrinology-journals.org
DOI: 10.1530/ERC-12-0207

Published by Bioscientifica Ltd.